

Global polarization of Λ and Ξ hyperons in Au+Au collisions in the STAR experiment

E. V. Alpatov (for the STAR Collaboration)^{1,*}

¹*National Research Nuclear University MEPhI*

Global polarization of Λ hyperons appearing in non-central heavy-ion collisions was measured by the STAR experiment at RHIC for Au+Au collisions with $\sqrt{s_{NN}} = 3 - 200$ GeV and at the LHC for Pb+Pb collisions with $\sqrt{s_{NN}} = 2.76$ and 5.02 TeV. Global polarization reflects its vortical nature of quark-gluon matter at its initial evolution stage.

Global polarization of multistrange hyperons, such as Ξ , can provide new information on hydrodynamic description of the system and its vorticity nature. In these proceedings, we will report results of Ξ and Λ global polarization for Au+Au collisions at $\sqrt{s_{NN}} = 19.6, 27, \text{ and } 54.4$ GeV.

I. INTRODUCTION

Relativistic hydrodynamics predicts that quark-gluon plasma, hot-dense matter produced in relativistic heavy-ion collisions, possess large vorticity in non-central collisions. It manifests itself in polarization of produced particles along the direction of vorticity. One can obtain polarization of hyperons from its parity violating weak decay properties [1, 2].

In the hyperon decays, the angular distribution of daughter baryon in the parent hyperon rest frame is given by:

$$\frac{dN}{d\cos\theta^*} \propto 1 + \alpha_H P_H \cos\theta^*, \quad (1)$$

α_H is the hyperon decay parameter, P_H is the hyperon polarization, $\cos\theta^*$ is the angle between the polarization vector and daughter baryon momentum in the hyperon rest frame [3].

Global polarization can be measured in respect to reaction plane (which is defined by the beam direction and impact parameter vector):

* egroker1@gmail.com

$$P_H = \frac{8}{\pi\alpha_H} \frac{\langle \sin(\Psi_1^{obs} - \phi_{daughter}^*) \rangle}{Res(\Psi_1)}, \quad (2)$$

16 where $\phi_{daughter}^*$ is the azimuthal angle of the daughter baryon in the parent hyperon rest
 17 frame, $Res(\Psi_1)$ is event plane resolution. Decay parameter values are $\alpha_\Lambda = 0.732 \pm 0.014$,
 18 $\alpha_{\bar{\Lambda}} = -0.758 \pm 0.010$, $\alpha_{\Xi^-} = -\alpha_{\Xi^+} = -0.401 \pm 0.010$ [4].

19 Global polarization of Λ hyperons was observed by the STAR for collision energies
 20 $\sqrt{s_{NN}} = 3 - 200$ GeV [5–8] and was described successfully by transport and hydrodynamic
 21 model calculations. Measurements of multistrange hyperon’s global polarization could pos-
 22 sibly achieve goal of understanding the nature of vorticity [9].

23 Λ hyperons are reconstructed via its decay $\Lambda \rightarrow p + \pi^-$, and for Ξ hyperons decay
 24 channel $\Xi^- \rightarrow \Lambda + \pi^-$ is analyzed. This cascade decay provides opportunity to measure
 25 its global polarization in two separate ways. One can use Equation 2 directly measuring
 26 angle of daughter Λ decaying from Ξ . Additionally, Ξ global polarization could transfer into
 27 its daughter Λ polarization with transfer factor $C_{\Xi-\Lambda} = 0.932$ and global polarization of Ξ
 28 hyperons could be measured by examining its daughter Λ global polarization [10–12].

29 In this proceedings we report on the measurements of the global polarization of $\Xi^- + \Xi^+$
 30 hyperons in Au+Au collisions at $\sqrt{s_{NN}} = 27, 54.4, \text{ and } 200$ GeV and compare them to those
 31 of $\Lambda + \bar{\Lambda}$.

32 II. DATA ANALYSIS

33 Data of Au+Au collisions at $\sqrt{s_{NN}} = 27$ and 54.4 GeV collected by STAR experiment
 34 was used for this analysis. STAR features cylindrical geometry detector for high-multiplicity
 35 collisions [13]. Events that passed minimum-bias trigger, with collision vertex within 70 cm
 36 along the beam axis from the center of Time-Projection Chamber (TPC) [14] and with
 37 vertex position within 2 cm from the beam line in the transverse plane were analyzed.

38 To reconstruct hyperons one needs daughter charged particle tracks that were measured
 39 in TPC within a pseudorapidity range $|\eta| < 1$ and with full azimuthal acceptance. Tracks
 40 with momentum above 0.15 GeV/c were identified via ionization energy losses, dE/dx , and
 41 by their squared mass obtained by TOF (Time-Of-Flight) [15]. Identified protons and pions
 42 were used for hyperon reconstruction.

43 Λ hyperons were reconstructed via topology of its decay $\Lambda \rightarrow p + \pi^-$ ($\bar{\Lambda} \rightarrow \bar{p} + \pi^+$), and

44 after Λ hyperons were obtained, the same procedure was performed for decays $\Xi^- \rightarrow \Lambda + \pi$
 45 ($\bar{\Xi}^+ \rightarrow \bar{\Lambda} + \pi^+$). Hyperon reconstruction was performed with KFPParticleFinder package [16].

46 The collision centrality was determined based on the measured multiplicity of charged
 47 tracks within midrapidity region. Centrality and trigger efficiency were obtained by fitting
 48 it to a Monte Carlo Glauber simulation.

49 For event plane reconstruction, EPD [17] ($2.1 < \eta < 5.1$) and BBC [18] ($3.3 < \eta < 5.1$)
 50 were used separately for $\sqrt{s_{NN}} = 27$ GeV, ZDC [19] ($\eta > 5.2$) and BBC for $\sqrt{s_{NN}} =$
 51 54.4 GeV collision energy. The first-order event plane, a proxy for reaction plane, was
 52 reconstructed using the spectator particles.

53 Global polarization measurements include correction for event plane resolution. Resolu-
 54 tion was calculated via two-subevent method, with use of East (forward rapidity) and West
 55 (backward rapidity) detectors in combination.

56 Following Equation 2, $\langle \sin(\Psi_1 - \phi_{daughter}^*) \rangle$ should be measured. To differentiate signal
 57 of real hyperons from combinatoric pairs of its daughter candidates, so-called "event-plane
 58 method" was used. This method consists in measuring number of hyperons as a function
 59 of $(\Psi_1 - \phi_{daughter}^*)$, and then fitting it with Fourier function to obtain the sine coefficient
 60 $\langle \sin(\Psi_1 - \phi_{daughter}^*) \rangle$.

61 III. RESULTS

62 Figure 1 presents global polarization of $\Lambda + \bar{\Lambda}$ and $\Xi^- + \bar{\Xi}^+$ hyperons as a function of
 63 collision energy for the centrality 20-50% (20-80% for $\Xi^- + \bar{\Xi}^+$ at $\sqrt{s_{NN}} = 200$ GeV due
 64 to smaller signal). Results of this analysis are shown together with $\sqrt{s_{NN}} = 7.7-200$ GeV
 65 Λ global polarization results and preliminary results for new data at $\sqrt{s_{NN}} = 27$ and 54.4
 66 GeV and the first $\sqrt{s_{NN}} = 200$ GeV study of Ξ global polarization. Theoretical calculations
 67 obtained from AMPT model [20] are shown together with the experimental results.

68 Global polarization was measured for Ξ hyperons directly via the angle of daughter Λ
 69 and via its daughter Λ decays considering the polarization transfer. Both measurements are
 70 consistent within large uncertainties.

71 Experimental trend for Ξ global polarization is consistent with AMPT calculations.
 72 Within uncertainties it is also consistent with Λ global polarization which could indicate
 73 the same nature of this phenomena for both particle species as expected.

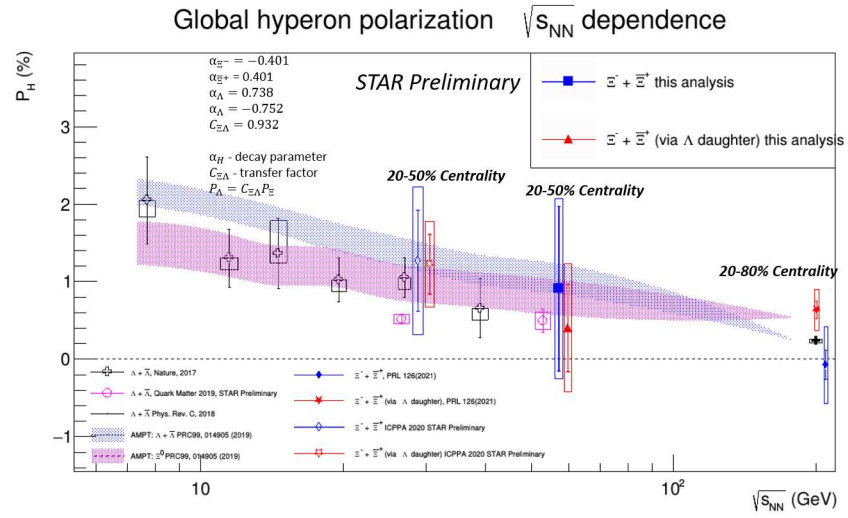


FIG. 1. Collision energy dependence of global polarization of hyperons in Au+Au collisions.

-
- 74 [1] Z.-T. Liang and X.-N. Wang, Phys. Rev. Lett. **94**, 102301 (2005).
- 75 [2] S. A. Voloshin, (2004), arXiv:nucl-th/0410089 [nucl-th].
- 76 [3] S. A. Voloshin and T. Niida, Phys. Rev. C **94**, 021901 (2016).
- 77 [4] P. A. Zyla *et al.* (Particle Data Group), Prog. Theor. and Exp. Phys. **2020**
78 (2020), 10.1093/ptep/ptaa104, 083C01, [https://academic.oup.com/ptep/article-](https://academic.oup.com/ptep/article-pdf/2020/8/083C01/34673722/ptaa104.pdf)
79 [pdf/2020/8/083C01/34673722/ptaa104.pdf](https://academic.oup.com/ptep/article-pdf/2020/8/083C01/34673722/ptaa104.pdf).
- 80 [5] B. I. Abelev and others., Phys. Rev. C **76** (2007), 10.1103/physrevc.76.024915.
- 81 [6] L. Adamczyk and et al., Nature **548**, 62–65 (2017).
- 82 [7] M. S. Abdallah *et al.* (STAR Collaboration), Phys. Rev. C **104**, L061901 (2021).
- 83 [8] L. Adamczyk and et al., Phys. Rev. C **98** (2018), 10.1103/physrevc.98.014910.
- 84 [9] J. Adam and et al. (STAR Collaboration), Phys. Rev. Lett. **126**, 162301 (2021).
- 85 [10] T. D. Lee and C. N. Yang, Phys. Rev. **108**, 1645 (1957).
- 86 [11] M. Huang *et al.* (HyperCP), Phys. Rev. Lett. **93**, 011802 (2004).
- 87 [12] K. B. Luk *et al.*, Phys. Rev. Lett. **85**, 4860–4863 (2000).
- 88 [13] M. Anerella *et al.*, Nucl. Instrum. Methods Phys. Res. Sect. A **499**, 280 (2003).
- 89 [14] M. Anderson *et al.*, Nucl. Instrum. Methods Phys. Res. Sect. A **499**, 659–678 (2003).
- 90 [15] W. Llope, Nucl. Instrum. Methods Phys. Res. Sect. A **661**, S110 (2012), x. Workshop on
91 Resistive Plate Chambers and Related Detectors (RPC 2010).
- 92 [16] Z. Maxim, Ph.D. thesis, Johann Wolfgang Goethe-367 Universitat (2016).
- 93 [17] J. Adams *et al.*, Nucl. Instrum. Methods Phys. Res. Sect. A **968**, 163970 (2020).
- 94 [18] C. A. Whitten (STAR), AIP Conf. Proc. **980**, 390 (2008).
- 95 [19] Y.-F. Xu, J.-H. Chen, Y.-G. Ma, A.-H. Tang, Z.-B. Xu, and Y.-H. Zhu, Nucl. Sci. Tech. **27**,
96 126 (2016).
- 97 [20] D.-X. Wei, W.-T. Deng, and X.-G. Huang, Phys. Rev. C **99**, 014905 (2019).